

# Effect of CO<sub>2</sub> partial pressure on oxidation of low-oxygen SiC fibers (Hi-Nicalon) in Ar-CO<sub>2</sub> gas mixtures

T. SHIMOO, K. OKAMURA

*Department of Metallurgy and Materials Science, Graduate School of Engineering, Osaka Prefecture University, 1-1, Gakuen-cho, Sakai, 599-8531 Osaka, Japan*

T. MORITA

*Osaka Gas Co., Ltd., 4-1-2, Hirano-machi, Chuo-ku, 541-0046 Osaka, Japan*

The oxidation behavior and thermal stability of Si–C fibers (Hi-Nicalon) in Ar-CO<sub>2</sub> gas mixtures were investigated at 1773 K, through mass change determination, XRD analysis, resistivity measurement, SEM observation and tensile tests. Mass gain and cristobalite formation were observed at  $p_{\text{CO}_2} \geq 10^3$  Pa, showing the occurrence of passive-oxidation of the fibers. On the other hand, the active-oxidation was characterized by the mass loss, no formation of SiO<sub>2</sub> film and a marked increase in resistivity at  $p_{\text{CO}_2} \leq 5 \times 10^2$  Pa. The oxygen potential for the active-to-passive oxidation transition in Ar-CO<sub>2</sub> gas mixtures was nearly identical to that in Ar-O<sub>2</sub> gas mixtures. About 50% of the strength in the as-received state was retained after the active-oxidation in Ar-CO<sub>2</sub> gas mixtures.

© 2004 Kluwer Academic Publishers

## 1. Introduction

Polycarbosilane-derived silicon carbide fibers are of great importance as reinforcing materials of ceramic matrix composites (CMC) for high-temperature applications. The high-temperature stability and oxidation resistance are required for fabrication and service of such fiber-reinforced CMC. Therefore, the microstructure, microchemistry, mechanical properties and thermal stability have been extensively investigated for the silicon carbide fibers after high-temperature exposure in inert environments (Ar, N<sub>2</sub> and vacuum) and oxidizing environments (O<sub>2</sub> and air). The combustion environments have been changed over a wide range of oxygen potentials. As a result, silicon carbide fibers can be oxidized in either the passive-oxidation regime or the active-oxidation regime. Since the passive-oxidation allows the surface of silicon carbide fibers to be coated with a stable SiO<sub>2</sub> film under high oxygen potential, further oxidation can be retarded. On the other hand, the active-oxidation causes the evaporation of SiC in the fibers producing SiO gas under a low oxygen potential, resulting in a marked degradation of fiber strength. While there were numerous reports on the passive-oxidation of silicon carbide fibers [1–21], there was little information on the active-oxidation of silicon carbide fibers. The authors have investigated the oxidation behaviors for various types of polymer-derived silicon carbide fibers in Ar-O<sub>2</sub> gas mixtures ranging from active-oxidation to passive-oxidation region [22–24]. CO<sub>2</sub> gas is necessarily present in the combustion environments. Therefore, further investigations of the oxidation of silicon carbide fibers throughout a wide

range of CO<sub>2</sub> concentrations are important. Therefore, the oxidation of Nicalon and Hi-Nicalon fibers (Nippon Carbon Co., Japan) has been studied in pure CO<sub>2</sub> gas [25, 26]. The exposure of the fibers at 1773 K in CO<sub>2</sub> gas showed the mass gain and silica formation which are characteristic of passive-oxidation. The reduction in CO<sub>2</sub> partial pressure appears to cause the transition from passive-oxidation to active-oxidation. In the present work, the CO<sub>2</sub> partial pressures were controlled by diluting CO<sub>2</sub> gas with Ar gas. The oxidation behavior of Hi-Nicalon fibers at 1773 K under CO<sub>2</sub> partial pressures from 10<sup>2</sup> to 10<sup>5</sup> Pa was studied through mass change determination, X-ray diffraction analysis, resistivity measurements, scanning electron microscopic observation and tensile tests. The CO<sub>2</sub> partial pressure for the active-to-passive oxidation transition was determined for Hi-Nicalon in Ar-CO<sub>2</sub> gas mixtures. These results were compared with those for the oxidation of Hi-Nicalon in Ar-O<sub>2</sub> gas mixtures [23].

## 2. Experimental method

The samples employed in this study were Si–C fibers (Hi-Nicalon) manufactured by Nippon Carbon Co. (Tokyo, Japan). Hi-Nicalon fibers have a molar composition of SiC<sub>1.39</sub>O<sub>0.01</sub> and a mean diameter of 14 μm. 500 mg of fibers, 3 cm in length, were charged in a high-purity alumina boat and then were placed in a alumina tube of an SiC resistance furnace. After evacuation, an Ar-CO<sub>2</sub> gas mixture was allowed to flow in to the tube at a flow rate of 100 cm<sup>3</sup>/min. The partial pressure of carbon dioxide was changed over a range from

$10^2$  to  $10^5$  Pa ( $p_{\text{Ar}} = 0$  Pa). The sample was heated at a rate of 300 K/min and after holding of 36 ks at 1773 K, it was cooled to room-temperature at 600 K/h.

The mass change of the fibers was determined by weighing before and after oxidation in Ar-CO<sub>2</sub> gas mixtures. The existing phases and  $\beta$ -SiC crystallite size of the fibers were determined by X-ray diffractometer (XRD). Before the specific resistivity measurements and tensile tests, SiO<sub>2</sub> film was removed with NH<sub>4</sub>OH + HF solution. The fibers oxidized in the active-oxidation region, as it is, were subjected to resistivity measurement and tensile test. The resistivity measurements were performed at room temperature by applying a direct current to a single fiber. Both ends of a fibers were attached, with an electroconductive resin, to copper electrode plates spaced 0.8 mm apart. Ten fibers were tested to determine the average resistivity. Room-temperature tensile tests were conducted using a 10 mm gauge length and a crosshead speed of 2 mm/min. The average of 10 tensile tests was taken as the tensile strength under each oxidation. Morphologies of as-oxidized fibers and SiO<sub>2</sub>-removed fibers were examined by field-emission scanning microscopy (FE-SEM).

### 3. Results

#### 3.1. Mass change

Fig. 1 shows the mass changes for Hi-Nicalon fibers oxidized for 36 ks at  $T = 1773$  K and  $p_{\text{CO}_2} = 10^2$ – $10^5$  Pa. There were the mass gains of +5–+7% at  $p_{\text{CO}_2} \geq 10^3$  Pa. Hi-Nicalon fibers were oxidized in the passive-oxidation regime in pure CO<sub>2</sub> gas (at  $p_{\text{CO}_2} = 10^5$  Pa) [25]. Therefore, the observed mass gains show the occurrence of passive-oxidation as well. On the other hand, the mass losses of about –5% were observed at  $p_{\text{CO}_2} \leq 5 \times 10^2$  Pa. These values are significantly lower than the mass loss of –0.5% after exposure of 36 ks at  $T = 1773$  K and  $p_{\text{Ar}} = 10^5$  Pa (in pure Ar gas). Furthermore, they were roughly double the mass loss of –2.3% for complete decomposition of amorphous silicon oxycarbide (SiC<sub>X</sub>O<sub>Y</sub>) phase in Hi-

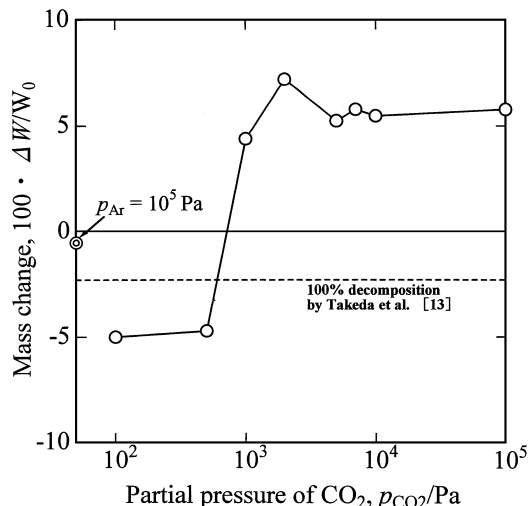


Figure 1 Mass changes for Hi-Nicalon fibers exposed for 36 ks at 1773 K in Ar-CO<sub>2</sub> gas mixtures.

Nicalon fibers [13]. This result implies that the high-temperature exposure in Ar-CO<sub>2</sub> gas mixtures with low CO<sub>2</sub> partial pressures caused the thermal decomposition of SiC<sub>X</sub>O<sub>Y</sub> phase and the subsequent active-oxidation of SiC grains, as well as the exposure in Ar-O<sub>2</sub> gas mixtures of  $p_{\text{CO}_2} \leq 10$  Pa [23].

#### 3.2. X-ray diffraction analysis

Fig. 2 shows the X-ray diffraction patterns for the fibers oxidized for 36 ks at  $T = 1773$  K and  $p_{\text{CO}_2} = 0$ – $10^5$  Pa. The sharp X-ray diffraction peak at  $2\theta \doteq 22^\circ$  reveals that Hi-Nicalon fibers were passively oxidized at  $p_{\text{CO}_2} \geq 10^3$  Pa, resulting in the formation of a cristobalite film on the fiber surface. On the other hand, in view of the mass loss (Fig. 1), no detection of cristobalite phase implies the occurrence of active-oxidation at  $p_{\text{CO}_2} \leq 5 \times 10^2$  Pa.

The apparent crystallite size of  $\beta$ -SiC,  $D_{\text{SiC}}$  was calculated from the half-width value of (111) peak using Scherrer's formula. Fig. 3 shows the value  $D_{\text{SiC}}$  shows a function of  $p_{\text{CO}_2}$ . The fibers after oxidation at 1773 K have three times larger  $\beta$ -SiC crystallite size ( $D_{\text{SiC}} \doteq 14$  nm) than the as-received fibers, independently on  $p_{\text{CO}_2}$ . The grain growth  $\beta$ -SiC is thought to be mainly caused by the crystallization of uncrystallized Si–C phase in Hi-Nicalon fibers ( $T \geq 1473$  K) [27]. Thus, Fig. 3 reveals that the oxidation temperature is a controlling factor in the grain growth of  $\beta$ -SiC.

#### 3.3. Fiber morphology

Fig. 4 show the morphologies of the fibers oxidized for 36 ks at 1773 K. All the fibers oxidized in the passive-oxidation region were coated with thick cristobalite film (A–F). The cristobalite film is known to crack during cooling, owing to a large volume shrinkage associated to the cristobalite  $\beta \rightarrow \alpha$  transition (A and C). Therefore, it is noted that no crack was observed in the cristobalite film formed at  $p_{\text{CO}_2} = 10^3$  Pa (E). On the other hand, the fracture appearance of unoxidized cores is smooth and glassy (B, D and F). The fiber surface is slightly roughened after exposure at  $p_{\text{CO}_2} = 5 \times 10^2$  Pa (G, H). A further reduction in  $p_{\text{CO}_2}$  value ( $p_{\text{CO}_2} = 10^2$  Pa) results in a peculiar appearance on fiber surface. As a consequence of active-oxidation, the grooves are deeply scooped in the surface of fiber (I, J). The fiber core displays a glassy fracture surface, as well as that oxidized in the passive-oxidation region, showing that the active-oxidation advances from the surface to the interior.

SEM photos at high magnification are shown in Fig. 5, for the fibers in the as-received state and after active-oxidation. The irregularity of the surface is very weak in the as-received state (A). The active-oxidation, as a consequence of the gasification of SiC grains, causes serious unevenness of fiber surface (B, C).

#### 3.4. Specific resistivity

Fig. 6 shows the specific resistivity of the fibers oxidized for 36 ks at  $T = 1773$  K as a function of  $p_{\text{CO}_2}$ . For the fibers oxidized at  $p_{\text{CO}_2} \geq 10^3$  Pa, a cristobalite

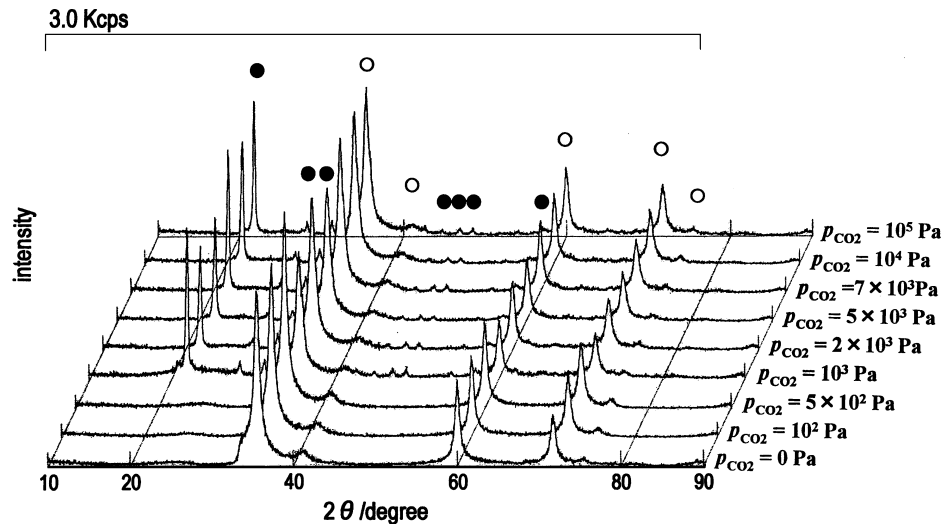


Figure 2 X-ray diffraction patterns for as-received fiber and fibers oxidized for 36 ks at 1773 K in Ar-CO<sub>2</sub> gas mixtures with different CO<sub>2</sub> partial pressures.

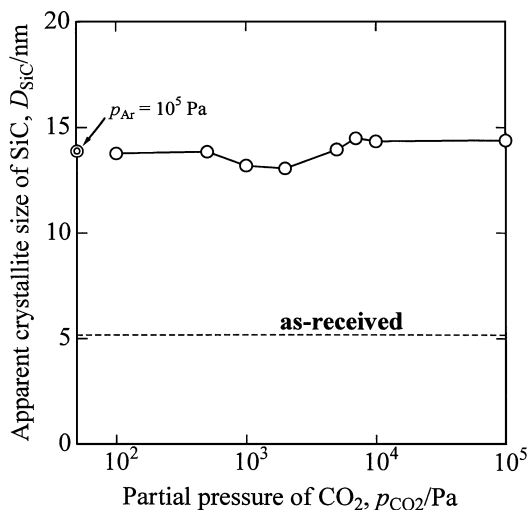


Figure 3  $\beta$ -SiC crystallite size of fibers heated for 36 ks at 1773 K in Ar-CO<sub>2</sub> gas mixtures with different CO<sub>2</sub> partial pressures.

film was removed with NH<sub>4</sub>F + HF solution before resistivity measurement. The resistivity of unoxidized core after passive-oxidation at  $p_{\text{CO}_2} \geq 10^3$  Pa is lowered to about half of that for the as-received fibers. This appears to be responsible for the organization of free carbon and the crystallization of Si-C phase in the fibers at  $T = 1773$  K [9, 27]. On the other hand, after active-oxidation region at  $p_{\text{CO}_2} \leq 5 \times 10^2$  Pa, the resistivity was larger than that in the as-received state. This is because the activation-oxidation renders the fiber structure highly porous, resulting in hindrance to the electrical conduction in a fiber. In addition, such high porosity of the fibers leads to a marked reduction of cross-sectional area controlling the conductivity. Therefore, the net resistivity of the fibers oxidized in the active-oxidation regime is thought to be overestimated by the use of apparent cross-sectional area calculated from the fiber diameter.

### 3.5. Tensile strength

Fig. 7 shows the room-temperature tensile strength for the fibers after oxidation of 36 ks at 1773 K,

as a function of  $p_{\text{CO}_2}$  value. The fibers oxidized in the passive-oxidation region (at  $p_{\text{CO}_2} \geq 10^3$  Pa) were subjected to tensile tests after removal of a cristobalite film. About 90% of the strength in the as-received state (2.4 GPa) is retained after oxidation at  $p_{\text{CO}_2} \geq 7 \times 10^3$  Pa. This strength is much larger than that of the fibers exposed in Ar gas (1.7 GPa). The reduction of  $p_{\text{CO}_2}$  in the passive-oxidation region causes a marked degradation of strength from 2.4 GPa at  $p_{\text{CO}_2} = 7 \times 10^3$  Pa to 0.7 GPa at  $p_{\text{CO}_2} = 10^3$  Pa. After oxidation in Ar-CO<sub>2</sub> gas mixtures, about 50% of the strength in the as-received state is retained even in the active-oxidation region.

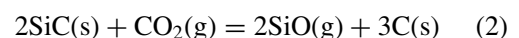
## 4. Discussion

The passive-oxidation rate of high-purity stoichiometric CVD-SiC in CO<sub>2</sub> gas was negligibly small and independent of temperature [28]. On the other hand, Hi-Nicalon fibers employed in this work were subjected to a severe passive-oxidation and showed strong temperature-dependence of oxidation rate [25]. At  $T = 1773$  K and  $p_{\text{CO}_2} \geq 10^3$  Pa, Hi-Nicalon fibers were passively oxidized in Ar-CO<sub>2</sub> gas mixtures, as well as pure CO<sub>2</sub> gas. A further reduction in CO<sub>2</sub> partial pressure to  $p_{\text{CO}_2} \leq 5 \times 10^2$  Pa caused the active-oxidation of Hi-Nicalon fibers. The oxidation of silicon carbide in CO<sub>2</sub> gas are given as follows [29]:

passive-oxidation,



active-oxidation,



The heat-treatment of Hi-Nicalon fibers in CO gas caused the formation of carbon film [30]. However, Auger electron spectroscopic analysis and X-ray diffraction show that no carbon film was formed on the surface of Hi-Nicalon fibers after oxidation in Ar-CO<sub>2</sub> gas mixtures. Therefore, it is necessary to consider alternative mechanism for the oxidation of Hi-Nicalon by CO<sub>2</sub> gas.

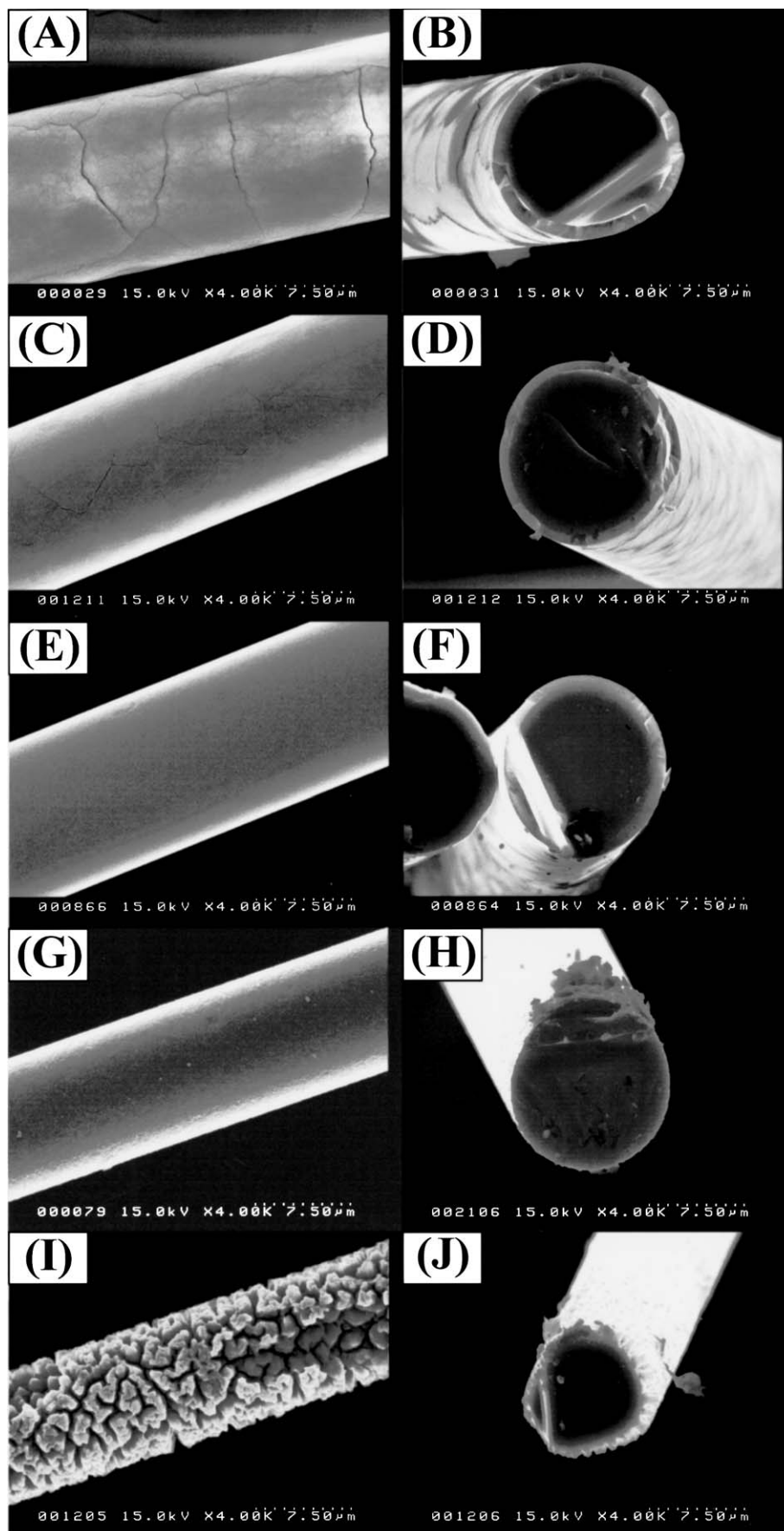


Figure 4 SEM photographs of fibres oxidized for 36 ks in Ar-CO<sub>2</sub> gas mixtures. (A), (B):  $p_{CO_2} = 10^5$  Pa, (C), (D):  $p_{CO_2} = 10^4$  Pa, (E), (F):  $p_{CO_2} = 10^3$  Pa, (G), (H):  $p_{CO_2} = 5 \times 10^2$  Pa, (I), (J):  $p_{CO_2} = 10^2$  Pa.

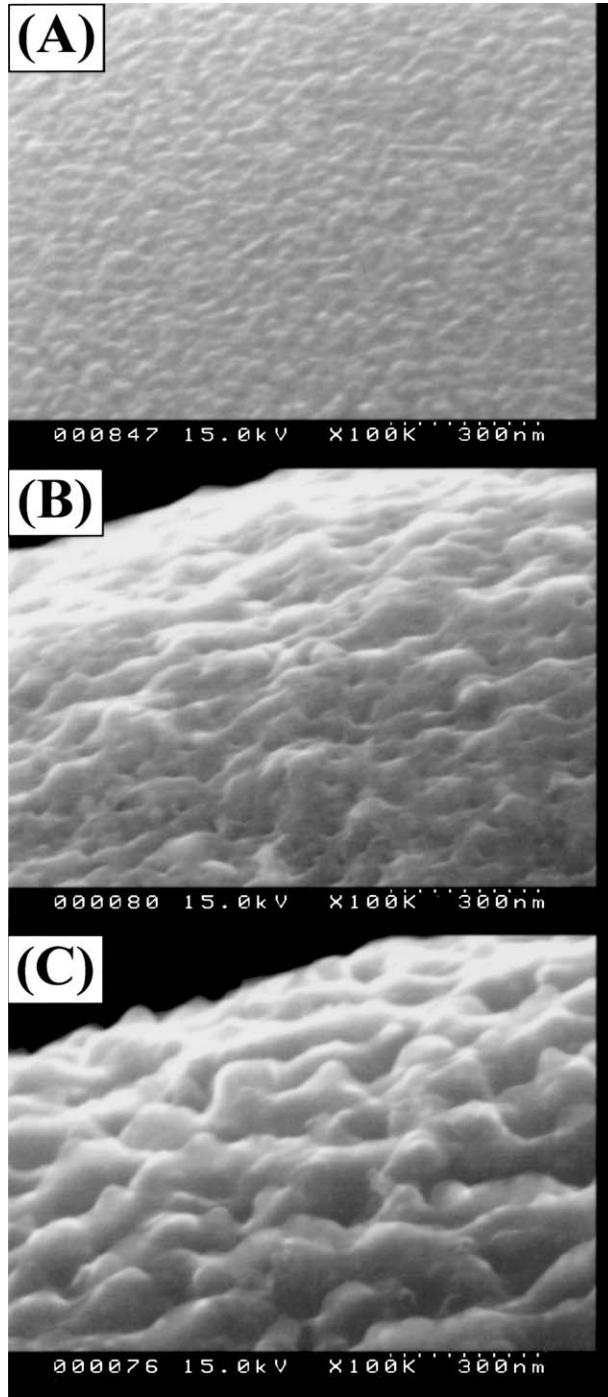
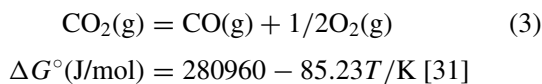


Figure 5 SEM photographs of as-received fiber (A) and fibers oxidized for 36 ks in Ar-CO<sub>2</sub> gas mixtures of  $p_{CO_2} = 5 \times 10^2$  Pa (B) and  $10^2$  Pa (C).

CO<sub>2</sub> gas dissociates to CO and O<sub>2</sub> gases at high temperatures.



Subsequently, Hi-Nicalon fibers are oxidized by dissociated oxygen:

in the passive-oxidation region:

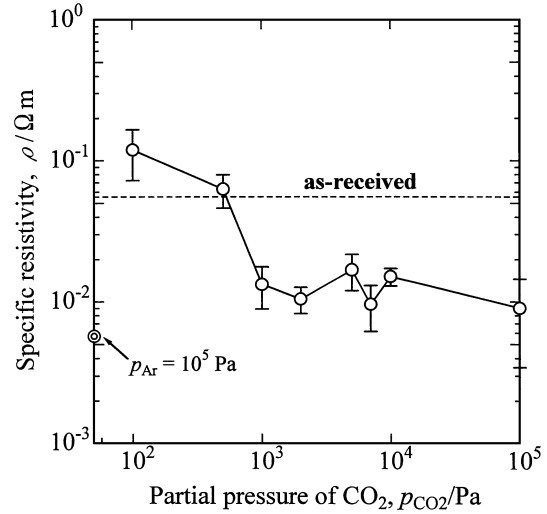
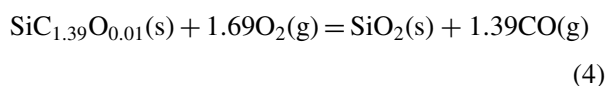


Figure 6 Specific resistivity of fibers heated for 36 ks at 1773 K in Ar-CO<sub>2</sub> gas mixtures with different CO<sub>2</sub> partial pressures.

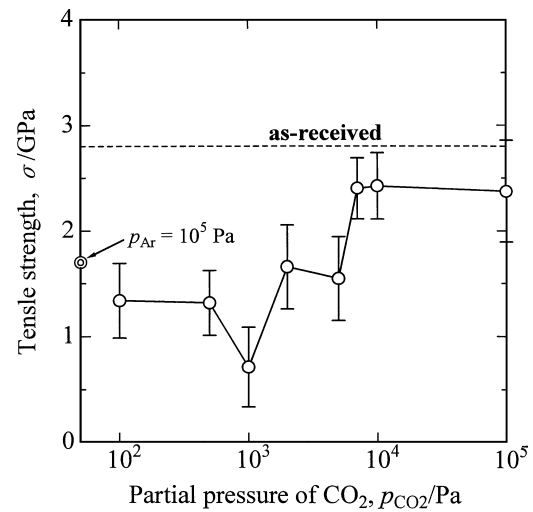
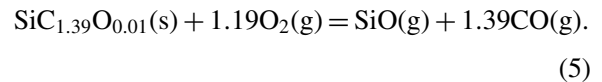


Figure 7 Room temperature tensile strength of fibers heated for 36 ks at 1773 K in Ar-CO<sub>2</sub> gas mixtures with different CO<sub>2</sub> partial pressures.

in the active-oxidation region:



The oxygen potentials of Ar-CO<sub>2</sub> gas mixtures,  $p_{O_2}$ , can be calculated from the standard free energy change,  $\Delta G^\circ$ , for the dissociation of CO<sub>2</sub> gas, i.e., reaction (1). Thus, on the basis of  $p_{O_2}$  values in gas mixtures, the properties of Hi-Nicalon fibers oxidized in Ar-CO<sub>2</sub> gas mixtures were compared with those of Hi-Nicalon fibers oxidized in Ar-O<sub>2</sub> gas mixtures [25].

Fig. 8 shows the mass change of Hi-Nicalon fibers oxidized for 36 ks at  $T = 1773$  K as a function of oxygen potential ( $p_{O_2}$ ) of Ar-CO<sub>2</sub> and Ar-O<sub>2</sub> gas mixtures. The mass gain caused by the passive-oxidation is smaller in Ar-CO<sub>2</sub> than in Ar-O<sub>2</sub> gas mixtures. This is partly due to different oxidation times; 36 ks for the oxidation in Ar-CO<sub>2</sub> gas mixtures, 72 Ks for that in Ar-O<sub>2</sub> gas mixtures. The mass change data displays that the transition from the mass gain to the mass loss occurred at  $p_{O_2} = 5-8$  Pa in Ar-CO<sub>2</sub> gas mixtures and at  $p_{O_2} = 10-25$  Pa in Ar-O<sub>2</sub> gas mixtures. Thus, the oxygen potential for the

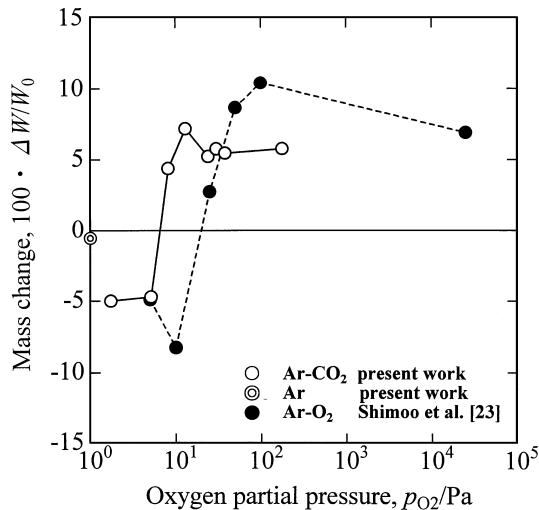


Figure 8 Mass change of Hi-Nicalon fibers heat-treated at 1773 K as function of oxygen potential of Ar-CO<sub>2</sub> and Ar-O<sub>2</sub> gas mixtures.

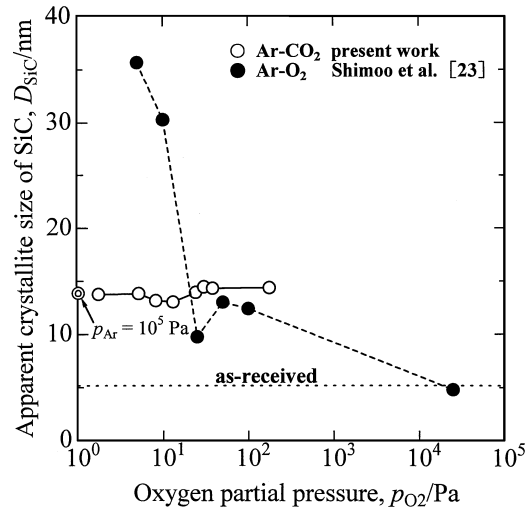


Figure 10 Relationship between apparent crystal size of  $\beta$ -SiC of Hi-Nicalon fibers oxidized at 1773 K and oxygen potential of gas mixtures.

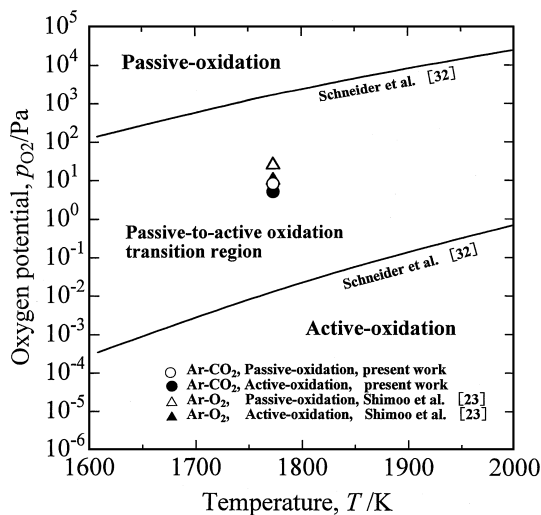


Figure 9 Oxygen potential of active-to-passive oxidation transition for different types of silicon carbide oxidized under various oxidation conditions [32] and for Hi-Nicalon fibers oxidized under Ar-CO<sub>2</sub> and Ar-O<sub>2</sub> gas mixtures.

active-to-passive oxidation transition is slightly lower in Ar-CO<sub>2</sub> than in Ar-O<sub>2</sub> gas mixtures. The active-to-passive oxidation transition is probably dependent not only on the oxidation temperature and oxygen partial pressure but also on the gas flow rate, physical properties of SiO<sub>2</sub> film and diffusivity of oxygen through the film. Therefore, the different oxygen potential for the active-to-passive oxidation transition between Ar-CO<sub>2</sub> than Ar-O<sub>2</sub> gas mixtures appears to be attributable to the difference in the experimental conditions. In addition, it is possible that CO<sub>2</sub> gas, as well as the dissociated oxygen, oxidizes Hi-Nicalon fibers in Ar-CO<sub>2</sub> gas mixtures.

Fig. 9 shows the active-to-passive oxidation transition region for different types of silicon carbide oxidized under various oxidation conditions [32]. The transition region is in the wide range of  $p_{O_2} = 10^{-2}$  to  $10^3$  Pa at 1773 K. The active-to-passive oxidation transition for Hi-Nicalon fibers oxidized in both Ar-CO<sub>2</sub> and Ar-O<sub>2</sub> gas mixtures are within this transition region for silicon carbides.

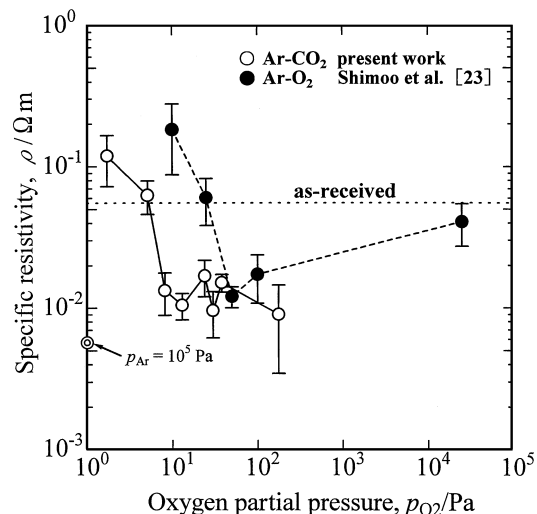


Figure 11 Relationship between specific resistivity of Hi-Nicalon fibers oxidized at 1773 K and oxygen potential of gas mixtures.

Fig. 10 shows the relationship between the apparent crystal size of  $\beta$ -SiC,  $D_{SiC}$ , and the oxygen potential ( $p_{O_2}$ ) of gas mixtures [23]. After oxidation in Ar-CO<sub>2</sub> and Ar-O<sub>2</sub> gas mixtures at 1773 K, the growth of SiC crystals was caused by the crystallization of noncrystallized Si-C phase and thermal decomposition of amorphous Si-C-O phase [27]. In particular, it may be noted that a marked coarsening of SiC grains ( $D_{SiC} = 30$ – $36$  nm) after the active-oxidation in Ar-O<sub>2</sub> gas mixtures of  $p_{O_2} \leq 10$  Pa. On the other hand, in Ar-CO<sub>2</sub> gas mixture, the  $D_{SiC}$  value after active-oxidation ( $p_{O_2} = 5$  Pa) was nearly identical to that after passive-oxidation.

Fig. 11 shows the relationship between the specific resistivity of Hi-Nicalon fibers,  $\rho$ , and the oxygen potential ( $p_{O_2}$ ) of gas mixtures [23]. The  $\rho$  value in the passive-oxidation region was lower than that in the as-received state, owing to the crystallization of SiC phase and the organization of carbon aggregates at 1773 K [9, 27]. The active-oxidation in both Ar-CO<sub>2</sub> and Ar-O<sub>2</sub> gas mixtures at 1773 K caused severe breakdown of fibrous structure, resulting in a 10-fold increase in specific resistivity.

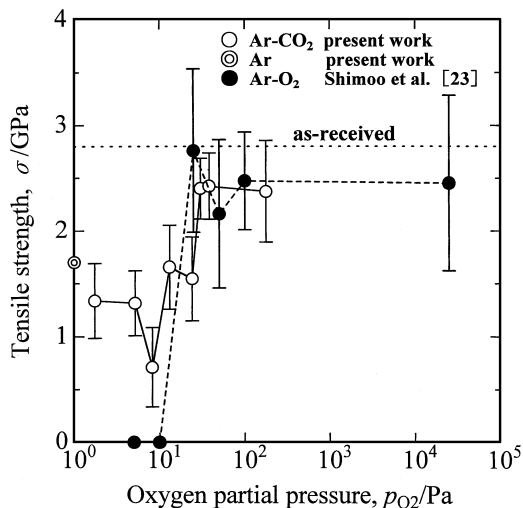


Figure 12 Relationship between room-temperature tensile strength of Hi-Nicalon fibers oxidized at 1773 K and oxygen potential of gas mixtures.

Fig. 12 shows the relationship between the room-temperature tensile strength of Hi-Nicalon fibers,  $\sigma$ , and the oxygen potential ( $p_{O_2}$ ) of gas mixtures [23]. 80–90% of the strength in the as-received state was retained after oxidation at  $p_{O_2} \geq 50$  Pa. There was a marked degradation of fiber strength after oxidation at  $p_{O_2} < 50$  Pa. The fiber strength was nearly completely lost after active-oxidation in Ar-O<sub>2</sub> gas mixtures ( $p_{O_2} \leq 10$  Pa). A drastic coarsening of SiC crystals during active-oxidation appears to be critical in the degradation of fiber strength. On the other hand, it may be noted that the fibers oxidized in Ar-CO<sub>2</sub> gas mixtures retained 48% of initial strength even after active-oxidation ( $p_{O_2} = 1.7$  Pa). As can be seen from Fig. 10, this is because the coarsening of SiC grains during active-oxidation was retarded in Ar-CO<sub>2</sub> gas mixtures.

## 5. Conclusion

The exposure of Hi-Nicalon fibers at 1773 K in Ar-CO<sub>2</sub> gas mixtures caused passive-oxidation which was characterized by mass gain and cristobalite formation at  $p_{CO_2} \geq 10^3$  Pa and the active-oxidation which was characterized by the mass loss and a marked increase in resistivity at  $p_{CO_2} \leq 5 \times 10^3$  Pa. The oxygen potential for the active-to-passive oxidation transition in Ar-CO<sub>2</sub> gas mixtures ( $p_{O_2} = 5$ –10 Pa) was slightly lower than that in Ar-O<sub>2</sub> gas mixtures ( $p_{O_2} = 10$ –25 Pa). While a marked coarsening of  $\beta$ -SiC grains was caused by the active-oxidation in Ar-O<sub>2</sub> gas mixtures ( $D_{SiC} = 30$ –36 nm),  $\beta$ -SiC grain size was almost identical throughout the active- and passive-oxidation region in Ar-CO<sub>2</sub> gas mixtures ( $D_{SiC} = 13$ –14 nm). Consequently, the fiber strength was completely lost after active-oxidation in Ar-O<sub>2</sub> gas mixtures but about 50% of the strength in the as-received state was retained after active-oxidation in Ar-CO<sub>2</sub> gas mixtures.

## References

1. T. MAH, N. L. HECHT, D. E. MCCULLUM, J. R. HOENIGMAN, H. M. KIM, A. P. KATZ and H. A. LIPSITT, *J. Mater. Sci.* **19** (1984) 1191.
2. Y. MANIETTE and A. OBERLIN, *ibid.* **24** (1989) 3361.
3. L. FILIPUZZI and R. NASLAIN, in Proceedings of 7th CIMTEC, Mater. Sci. Monograph 68 Adv. Structural Inorg. Composites, edited by P. Voncezini (Elsevier, Amsterdam, 1991) p. 35.
4. H.-E. KIM and A. J. MOORHEAD, *J. Amer. Ceram. Soc.* **74** (1991) 666.
5. Y. GOGOTSI and M. YOSHIMURA, *J. Mater. Sci. Lett.* **13** (1994) 680.
6. M. H. BERGER, N. HOCHET and A. R. BUNSELL, *J. Microsc.* **177** (1995) 230.
7. P. LE. COUSTOMER, M. MONTHIOUX and A. OBERLIN, *Br. Ceram. Trans.* **94** (1995) 177.
8. C. VIX-GUTERL and P. EHRBURGER, *J. Mater. Sci.* **31** (1996) 5363.
9. G. CHOLLON, R. R. PAILLER, R. NASLAIN, F. LAANANI, M. MONTHIOUX and P. PLY, *ibid.* **32** (1997) 327.
10. G. CHOLLON, M. CZERNIAK, R. PAILLER, X. BOURRAT, R. NASLAIN, J. P. PILLOT and R. CANNET, *ibid.* **32** (1997) 893.
11. M. H. BERGER, N. HOCHE and A. R. BUNSELL, *J. Microsc.* **185** (1997) 243.
12. Y. T. ZHU, S. T. TAYLOR, M. G. STOUT, D. P. BUTT and T. C. LOWE, *J. Amer. Ceram.* **81** (1998) 655.
13. M. TAKEDA, J. SAKAMOTO, Y. IMAI and H. ICHIKAWA, *Comp. Sci. Tech.* **59** (1999) 813.
14. T. SHIMOO, H. CHEN and K. OKAMURA, *J. Ceram. Soc. Jpn.* **100** (1992) 929.
15. T. SHIMOO, T. HAYATSU, M. TAKEDA, H. ICHIKAWA, T. SEGUCHI and K. OKAMURA, *ibid.* **102** (1994) 617.
16. T. SHIMOO, F. TOYODA and K. OKAMURA, *ibid.* **106** (1998) 447.
17. *Idem.*, *ibid.* **107** (1999) 263.
18. *Idem.*, *J. Mater. Sci.* **35** (2000) 3301.
19. *Idem.*, *J. Amer. Ceram. Soc.* **83** (2000) 1450.
20. *Idem.*, *J. Mater. Sci.* **35** (2000) 3811.
21. T. SHIMOO, H. TAKEUCHI, M. TAKEDA and K. OKAMURA, *J. Ceram. Soc. Jpn.* **108** (2000) 1096.
22. T. SHIMOO, Y. MORISADA and K. OKAMURA, *J. Amer. Ceram. Soc.* **83** (2000) 3049.
23. *Idem.*, *J. Mater. Sci.* **37** (2002) 1793.
24. *Idem.*, *ibid.* **37** (2002) 4361.
25. T. SHIMOO, T. MORITA and K. OKAMURA, *J. Amer. Ceram. Soc.* **84** (2001) 2975.
26. *Idem.*, *J. Mater. Sci.* **37** (2002) 3181.
27. M.-H. BERGER, N. HOCHET and A. R. BUNSELL, "Properties and Microstructures of Small-Diameter SiC-Based Fibers," in "Fine Ceramic Fibers," edited by A. R. Bunsell and M.-H. Berger (Marcel Dekker, New York, 1999) p. 246.
28. E. J. OPILA, *J. Amer. Ceram. Soc.* **81** (1998) 1949.
29. G. X. WANG, G. Q. LU and A. B. YU, *J. Mater. Sci.* **33** (1998) 1309.
30. T. SHIMOO, T. MORITA and K. OKAMURA, *ibid.* **38** (2003) in printing.
31. E. T. TURKDOGAN, "Physical Chemistry of High Temperature Technology" (Academic Publishers, New York, 1980) p. 1.
32. B. SCHNEIDER, A. GUETTE, R. NASLAIN, M. CATALDI and A. COSTECALDE, *J. Mater. Sci.* **33** (1998) 535.

Received 22 July  
and accepted 23 December 2003